Cell

Article

Supporting Aspartate Biosynthesis Is an Essential Function of Respiration in Proliferating Cells

Graphical Abstract

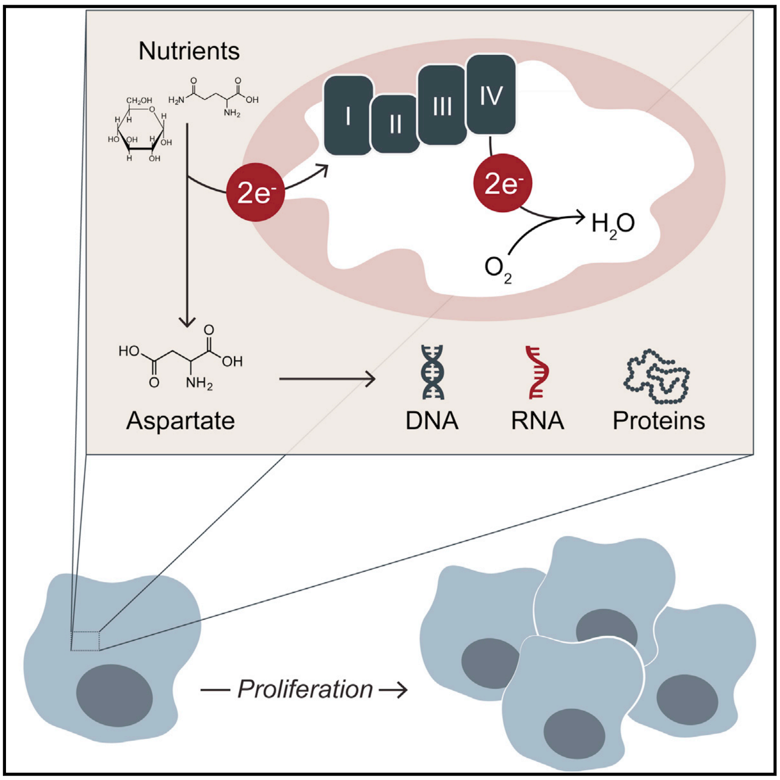

Highlights

- Electron acceptor deficiency limits respiration-deficient cell proliferation
- Electron acceptor α-ketobutyrate supports respiration-deficient cell proliferation
- Aspartate supports proliferation in the absence of electron acceptors
- A primary role of respiration in proliferating cells is to produce aspartate

Authors

Lucas B. Sullivan, Dan Y. Gui, Aaron M. Hosios, Lauren N. Bush, Elizaveta Freinkman, Matthew G. Vander Heiden

Correspondence

mvh@mit.edu

In Brief

A primary role of respiration in proliferating cells is to support aspartate synthesis.

Sullivan et al., 2015, Cell *162*, 552–563
July 30, 2015 ©2015 Elsevier Inc.
http://dx.doi.org/10.1016/j.cell.2015.07.017

CellPress

Supporting Aspartate Biosynthesis Is an Essential Function of Respiration in Proliferating Cells

Lucas B. Sullivan,[1,4] Dan Y. Gui,[1,4] Aaron M. Hosios,[1] Lauren N. Bush,[1] Elizaveta Freinkman,[2] and Matthew G. Vander Heiden[1,3,*]

[1]The Koch Institute for Integrative Cancer Research and Department of Biology, Massachusetts Institute of Technology, Cambridge, MA 02139, USA

[2]Whitehead Institute for Biomedical Research, Nine Cambridge Center, Cambridge, Massachusetts 02142, USA

[3]Dana-Farber Cancer Institute, Boston, MA 02115, USA

[4]Co-first author

*Correspondence: mvh@mit.edu

http://dx.doi.org/10.1016/j.cell.2015.07.017

SUMMARY

Mitochondrial respiration is important for cell proliferation; however, the specific metabolic requirements fulfilled by respiration to support proliferation have not been defined. Here, we show that a major role of respiration in proliferating cells is to provide electron acceptors for aspartate synthesis. This finding is consistent with the observation that cells lacking a functional respiratory chain are auxotrophic for pyruvate, which serves as an exogenous electron acceptor. Further, the pyruvate requirement can be fulfilled with an alternative electron acceptor, alpha-ketobutyrate, which provides cells neither carbon nor ATP. Alpha-ketobutyrate restores proliferation when respiration is inhibited, suggesting that an alternative electron acceptor can substitute for respiration to support proliferation. We find that electron acceptors are limiting for producing aspartate, and supplying aspartate enables proliferation of respiration deficient cells in the absence of exogenous electron acceptors. Together, these data argue a major function of respiration in proliferating cells is to support aspartate synthesis.

INTRODUCTION

In mammalian cells, mitochondrial respiration allows coupling of nutrient oxidation to ATP production. Respiration involves a series of redox reactions where electrons from a reduced substrate are ultimately transferred to molecular oxygen as the final electron acceptor. This results in oxidation of consumed nutrients and reduction of molecular oxygen to water. The free energy released from this series of oxidation-reduction reactions is coupled to production of an electrochemical gradient that can be used to drive ATP synthesis, membrane transport, and thermogenesis (Harms and Seale, 2013; Mitchell, 1961; Schleyer et al., 1982).

While supporting bioenergetics is a critical function of respiration in mammalian cells, many proliferating cells display increased fermentation, which alone can be sufficient to supply ATP (Gottlieb and Tomlinson, 2005). In contrast to most normal tissues, cancer cells consume increased amounts of glucose and metabolize much of this glucose to lactate even in the presence of ample oxygen (Koppenol et al., 2011; Warburg et al., 1924). This phenotype, termed aerobic glycolysis or the Warburg effect, was initially hypothesized to result from diminished mitochondrial function (Warburg, 1956). However, despite utilizing aerobic glycolysis, most cancer cells also consume oxygen (Weinhouse, 1956; Zu and Guppy, 2004). Notably, in cancer cell lines, the primary substrate for oxidation is often not glucose but rather glutamine, one of the most heavily consumed nutrients by cells in culture (Fan et al., 2013; Kovacević, 1971; Zielke et al., 1984). Thus, aerobic glycolysis likely does not replace mitochondrial respiration, but rather, in proliferating cells these processes occur in parallel.

Most cells that engage in aerobic glycolysis are not only capable of respiration, but also require respiration for proliferation. Exposure of cancer cells in culture to respiration inhibitors blocks proliferation (Harris, 1980; Howell and Sager, 1979; Kroll et al., 1983; Löffer and Schneider, 1982). In vivo, maintenance of mtDNA is required for autochthonous tumor formation (Weinberg et al., 2010), and inhibition of respiration suppresses tumor growth in xenografts (Wheaton et al., 2014; Zhang et al., 2014). These findings argue that mitochondrial respiration is essential for rapid proliferation, but whether respiration is advantageous for proliferation beyond producing ATP is less clear.

Despite the importance of respiration in mammalian cell proliferation, under specific culture conditions proliferation is possible even in the absence of respiration. Serial passage in low-dose ethidium bromide produces cells devoid of mtDNA (ρ^0 cells) (King and Attardi, 1989, 1996). ρ^0 cells lack a functional mitochondrial electron transport chain (ETC), and these respiration-incompetent cells fail to proliferate unless supra-physiological levels of uridine and pyruvate are present in the culture media (King and Attardi, 1989). Uridine auxotrophy is explained by the fact that the de novo pyrimidine biosynthesis enzyme dihydroorotate dehydrogenase (DHODH) transfers electrons directly to the ETC to convert dihydroorotate to orotate. Thus, loss of electron transport to O_2 prevents this reaction, and exogenous uridine is needed to produce pyrimidines (Grégoire et al., 1984). The requirement for pyruvate, however, was initially unexpected because cells deficient in mtDNA are highly glycolytic and capable of generating large amounts of pyruvate (King and Attardi, 1989).

The fact that adding specific nutrients can substitute for respiration suggests respiration fulfills specific metabolic requirements for proliferating cells. While ATP synthesis via oxidative phosphorylation is often assumed to be the critical output of respiration, neither exogenous uridine nor pyruvate can be oxidized to supply ATP in the absence of respiration. However, other than dihyroorotate to orotate conversion, the metabolic function(s) that become limiting for proliferation in the absence of respiration are unknown.

Here we show that loss of mitochondrial respiration causes proliferating cells to become functionally limited for electron acceptors. This lack of electron acceptors impairs de novo aspartate synthesis and inhibits proliferation. Strikingly, this proliferation block can be overcome by supplementing cells with exogenous electron acceptors or by high levels of aspartate. Taken together, our data argue that the most essential metabolic function for proliferation provided by mitochondrial respiration is to provide access to electron acceptors to support aspartate biosynthesis.

RESULTS

Alpha-Ketobutyrate Can Substitute for Pyruvate to Support Proliferation in Respiration-Incompetent Cells

Cells lacking a functional mitochondrial ETC require pyruvate for proliferation (King and Attardi, 1989). This suggests that pyruvate substitutes for an essential metabolic function of respiration. We reasoned that better understanding the role of pyruvate in these cells would allow us to gain insight into how respiration supports the metabolic needs of proliferating cells. To avoid respiration-independent effects of mtDNA depletion, we used 143B ρ^0 cells repopulated with mtDNA containing a frameshift deletion in cytochrome B (143B CytB) (Rana et al., 2000). 143B CytB cells have otherwise wild-type mitochondria, but are respiration-incompetent due to lack of cytochrome B in complex III and thus lack a functional ETC. As a control we utilized 143B ρ^0 cells which were repopulated with wild-type mtDNA (143B WT cybrid) and are respiration-competent with a functional ETC. 143B CytB cells are auxotrophic for pyruvate as they fail to proliferate in the absence of pyruvate (Figure 1A). Conversely, 143B WT cybrid cells cultured with or without pyruvate divide at a similar rate (Figure S1A), confirming that pyruvate auxotrophy accompanies loss of mitochondrial respiration.

Several hypotheses have been proposed to explain pyruvate auxotrophy (Howell and Sager, 1979; King and Attardi, 1996; Morais et al., 1994; van den Bogert et al., 1992). Pyruvate carbon

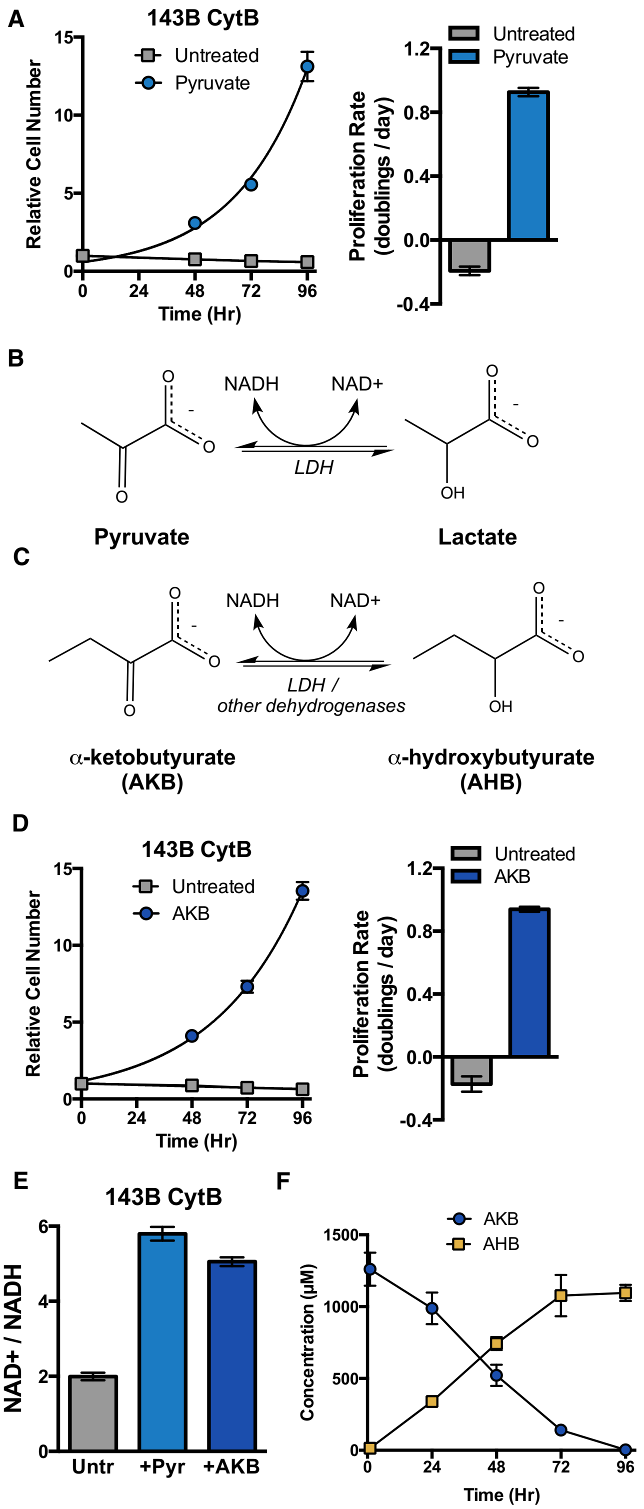

Figure 1. Cytochrome B Mutant 143B Cybrid Cells Are Auxotrophic for Electron Acceptors that Can Regenerate NAD+

(A) Proliferation rate of 143B CytB cells was determined in the presence or absence of pyruvate. (left) Cell counts, normalized to cell number at t = 0 when media conditions were applied, were assessed over time and used to calculate proliferation rate (right).

(B) Pyruvate is a substrate of lactate dehydrogenase (LDH), accepting electrons from NADH to produce NAD+ and lactate.

(C) Alpha-ketobutyrate (AKB) can also act as an electron acceptor from NADH and yield NAD+ and alpha-hydroxybutyrate (AHB).

(D) Proliferation rate for 143B CytB cells in the presence or absence of AKB was determined as in (A).

(E) Intracellular ratio of NAD+/NADH was determined in 143B CytB cells in untreated media or in the presence of pyruvate (Pyr) or AKB.

(F) The concentration of AKB and AHB in the media of 143B CytB cells cultured in the presence of AKB was determined over time by GCMS analysis. Values in all figure panels denote mean ± SEM, n = 3.

See also Figure S1.

has many metabolic fates, including conversion to oxaloacetate via pyruvate carboxylase, malate via malic enzyme, and acetyl-CoA via the pyruvate dehydrogenase complex. Thus, one hypothesis is that pyruvate acts as a carbon substrate for synthesis of biosynthetic intermediates that are normally dependent on respiration. An alternative hypothesis is that in the absence of functional ETC, cells cannot adequately oxidize cellular NADH. Hence, pyruvate is required as an exogenous electron acceptor to regenerate NAD+ via the lactate dehydrogenase (LDH) reaction (Figure 1B). Importantly, the continued production of pyruvate from glycolysis requires NAD+, and therefore, the use of glucose-derived pyruvate as a biosynthetic intermediate requires an exogenous source of NAD+ regeneration to maintain redox balance.

In order to decouple the potential roles of pyruvate, we sought alternative substrates that could support 143B CytB cell proliferation in the absence of pyruvate. One candidate we identified is the four-carbon metabolite alpha-ketobutyrate (AKB), which can act as a substrate for LDH or other intracellular dehydrogenases (Figure 1C). While not the preferred substrate for LDH, we confirmed that LDH can utilize AKB to regenerate NAD+ from NADH with reasonable kinetics (Figure S1B). We tested whether AKB is sufficient to support proliferation of 143B CytB cells in the absence of pyruvate. Indeed, AKB restores proliferation of 143B CytB cells to similar levels as cells cultured with pyruvate (Figure 1D). AKB addition does not restore oxygen consumption (Figure S1C), alleviate uridine auxotrophy (Figure S1D), or impact proliferation of 143B WT cybrids (Figure S1E), demonstrating that AKB acts similarly to pyruvate in supporting proliferation of respiration-deficient 143B CytB cells.

As exogenous electron acceptors, AKB and pyruvate are both expected to regenerate NAD+. We measured the NAD+/NADH ratios in 143B CytB cells cultured in the absence or presence of either pyruvate or AKB. Addition of either pyruvate or AKB is sufficient to increase the NAD+/NADH ratio, consistent with these molecules serving as electron acceptors (Figure 1E). Given that AKB and pyruvate have different metabolic carbon-fates, we hypothesized that AKB is used primarily as an electron acceptor and not as a carbon substrate in other metabolic pathways. When AKB is metabolized by a dehydrogenase that uses NADH to reduce the alpha-ketone to a hydroxyl and regenerate NAD+, the expected product is alpha-hydroxybutyrate (AHB) (Figure 1C). To test whether this is the fate of exogenous AKB in 143B CytB cells, we quantitatively measured the consumption of AKB and excretion of AHB in the media of 143B CytB cells cultured in the absence of pyruvate. We found that AKB consumption matched AHB excretion (Figure 1F). AKB and AHB are both four-carbon metabolites that differ only by oxidation state, and levels of these metabolites in the culture media are negligible when AKB is not added. Thus, this result strongly suggests that AKB acts only as an electron acceptor and does not directly contribute carbon to metabolism. To further confirm that pyruvate and AKB carbon are metabolized differently, we find that pyruvate, but not AKB, maintains viability of 143B WT cybrid and HeLa cells deprived of glucose and glutamine (Figure S1F). Since AKB is sufficient to replace pyruvate in supporting 143B CytB cell proliferation, the pyruvate auxotrophy of these respiration incompetent cells is best explained as a requirement for exogenous electron acceptors. Taken together, these data suggest that access to exogenous electron acceptors provided by respiration (O_2), pyruvate, or AKB are required to support proliferation.

Inhibition of Respiration Causes Auxotrophy for Electron Acceptors

Generation of 143B CytB cells involves a selection process that could result in uncharacterized changes that alter the metabolic requirements provided by respiration. To test whether parental cells with functional ETC have the same requirements for respiration, we treated wild-type 143B cells with an array of respiration inhibitors. Given the known DHODH requirement for respiration and the finding that AKB can substitute for pyruvate as an electron acceptor, this and all subsequent experiments were performed in the presence of uridine and in the absence of pyruvate. Inhibitors of mitochondrial complex I, complex III, complex IV, and ATP synthase were all sufficient to suppress proliferation and most resulted in decreased cell count over time (Figure 2A). Exposure to ETC inhibitors at these doses decreased oxygen consumption (Figure S2) and thus decreased access to electron acceptors. To determine if respiration is required for proliferation because it provides access to electron acceptors, we tested if AKB supplementation could restore proliferation. In all cases, AKB addition rescued proliferation to rates comparable to that of untreated cells (Figure 2A). To confirm that AKB also acts as an electron acceptor in this context, we measured the NAD+/NADH ratio in cells treated with ETC inhibitors in the absence or presence of AKB. All ETC inhibitors decreased cellular NAD+/NADH ratio in the absence of AKB (Figure 2B). AKB addition restored NAD+/NADH, while having no effect on O_2 consumption, confirming that AKB is sufficient to increase oxidized cofactor pools (Figures 2B and S2).

To determine if a similar dependence on respiration exists in other proliferating cells, we treated a panel of genetically diverse cell lines including both transformed and non-transformed cells with three representative respiration inhibitors: rotenone (complex I inhibitor), antimycin (complex III inhibitor), and oligomycin (ATP synthase inhibitor). For all cell lines, treatment with any of the inhibitors blocked proliferation, and AKB was sufficient to restore proliferation (Figure 2C).

The use of oxygen as a terminal electron acceptor by mitochondrial respiration is well described. However, this role for oxygen is classically considered in the context of enabling NADH oxidation by the ETC to produce a membrane potential across the mitochondrial inner membrane and support ATP synthesis. Notably, reduction of AKB allows regeneration of NAD+ but does not support ATP production, arguing that mitochondrial ATP production is not required for proliferation. To further test this idea, we utilized oligomycin, a specific ATP synthase inhibitor, and the ionophore carbonyl cyanide-4-(trifluoromethoxy) phenylhydrazone (FCCP), an uncoupler of the mitochondrial membrane potential. In normal respiration, electrons from NADH are transferred to the ETC and then ultimately to oxygen to generate an electrochemical proton gradient across the mitochondrial inner membrane, which can drive ATP synthesis. Oligomycin does not directly inhibit components of the ETC, but

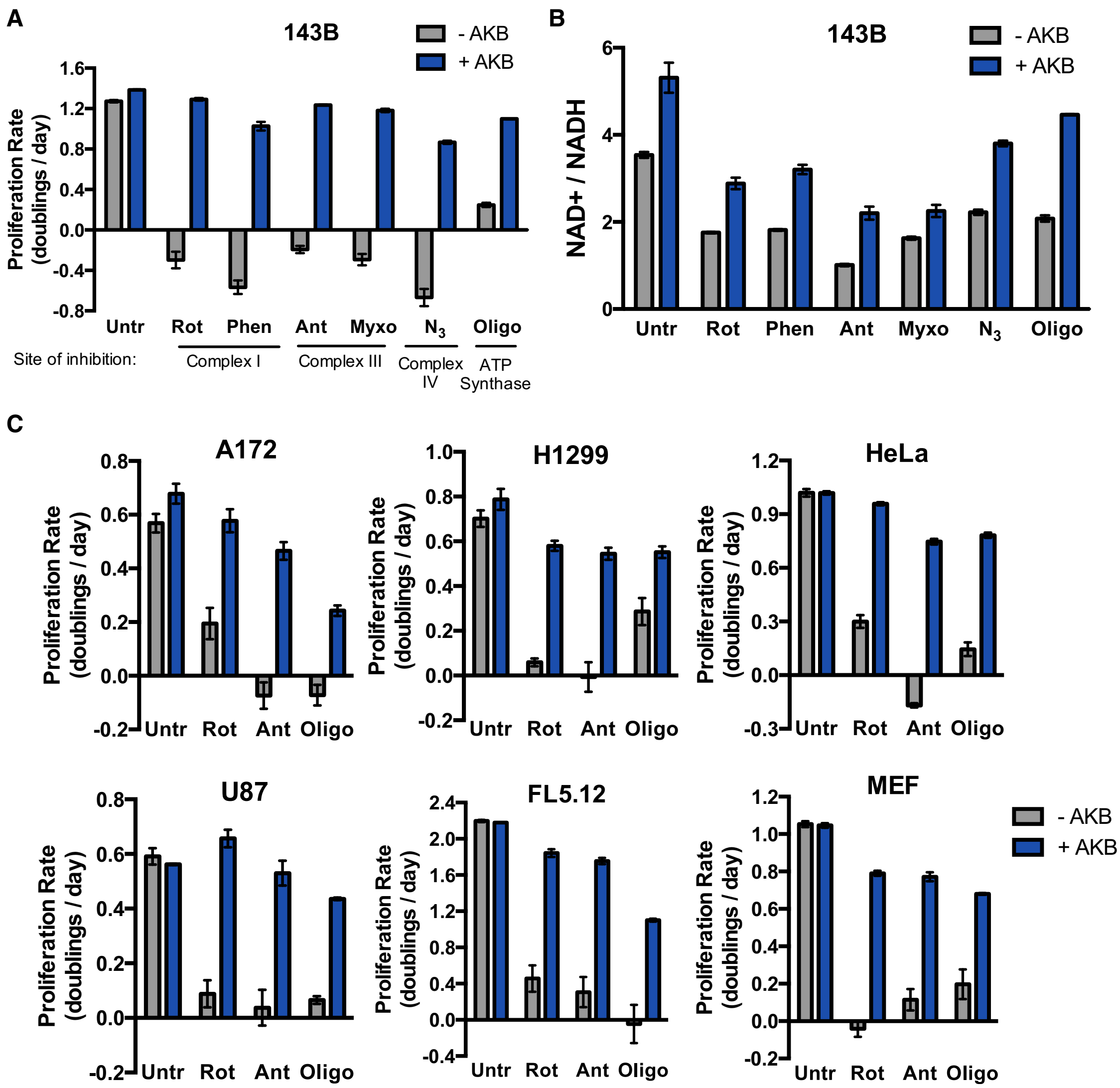

Figure 2. Proliferation of Respiration-Inhibited Cells Is Restored by Exogenous Electron Acceptors

(A) The proliferation rate of 143B cells was determined in media with or without AKB supplementation in the absence (Untr) or in the presence of the mitochondrial respiration inhibitors rotenone (Rot), phenformin (Phen), antimycin (Ant), myxothiazol (Myxo), azide (N_3), or oligomycin (Oligo).

(B) The ratio of NAD+/NADH was determined in 143B cells with or without AKB supplementation in the absence or presence of respiration inhibitors as in (A).

(C) The proliferation rate of A172, H1299, HeLa, U87, FL5.12, and MEF cell lines was determined with or without AKB supplementation in the absence or presence of rotenone, antimycin, or oligomycin. Values in all figure panels denote mean ± SEM, n = 3.

See also Figure S2.

rather slows ETC electron transfer to oxygen by hyperpolarizing the mitochondrial membrane potential (Figure 3A) (Brand and Nicholls, 2011). Thus, treatment with oligomycin alone decreases oxygen consumption (Figure S2C). However, addition of the uncoupling agent FCCP can restore the ability to transfer electrons from the ETC to oxygen in the presence of oligomycin by relieving membrane hyperpolarization without reversing inhibition of ATP synthase function (Figure 3A). Thus, if providing access to electron acceptors is the essential function of respiration independent of ATP production, restoring oxygen consumption with a low dose of FCCP that does not completely dissipate all intracellular proton membrane potentials should restore proliferation of oligomycin-treated cells. We compared the proliferation rate of 143B cells cultured in oligomycin in the absence or presence of low-dose FCCP. Consistent with the hypothesis, FCCP addition increased proliferation of oligomycin-treated cells (Figure 3B). Also in agreement with the hypothesis, FCCP increased both oxygen consumption and the NAD+/NADH ratio (Figures 3C and 3D). Since FCCP and oligomycin act independently, FCCP addition does not restore mitochondrial ATP production. These data argue that providing access to electron acceptors, rather than supporting mitochondrial ATP production, is a limiting function of mitochondrial respiration for supporting proliferation.

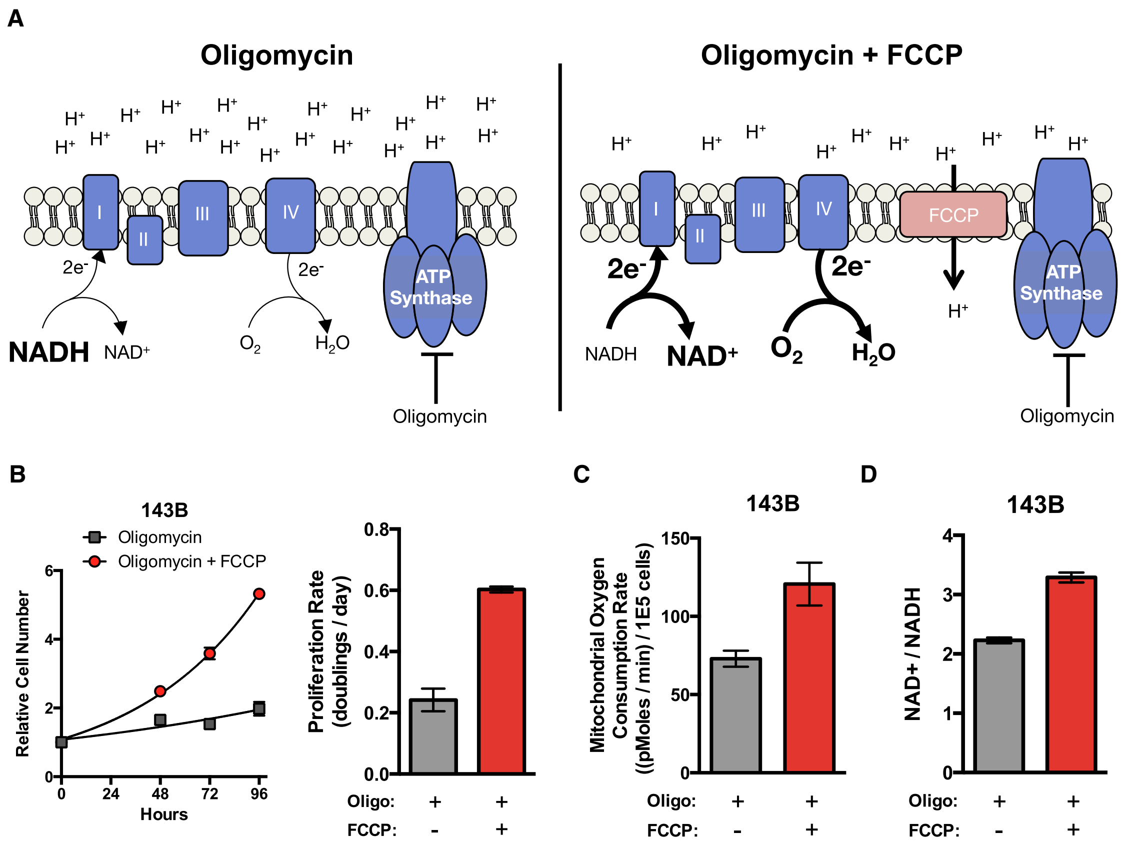

Figure 3. Oxygen Utilization in the Absence of Mitochondrial ATP Production is Sufficient for Cell Proliferation

(A) Schematic illustrating the effects of oligomycin and FCCP on mitochondrial membrane potential and ATP synthesis. Oligomycin treatment inhibits ATP synthase, resulting in a hyperpolarized mitochondrial membrane. This hyperpolarization inhibits proton pumping and thereby inhibits ETC activity resulting in decreased NADH oxidation and O_2 consumption (left). Treatment with FCCP in addition to oligomycin relieves the hyperpolarization of the mitochondrial membrane allowing restoration of NADH oxidation and mitochondrial O_2 consumption without restoring ATP production (right).

(B) Proliferation rate of 143B cells treated with oligomycin in the presence or absence of FCCP treatment.

(C) Mitochondrial oxygen consumption rate of 143B cells treated with oligomycin with or without FCCP.

(D) Intracellular NAD+/NADH ratio in 143B cells treated with oligomycin in the presence or absence of FCCP.

Values in all figure panels denote mean ± SEM, n = 3 (B and D), n = 5 (C).

Electron Acceptor Insufficiency Causes Inhibition of Nucleotide Biosynthesis

To gain mechanistic insight into why electron acceptors are required for proliferation, we characterized the phenotype of respiration incompetent cells under conditions where access to electron acceptors is limiting. Analysis of DNA content in non-proliferating 143B CytB cells without AKB suggested that these cells do not arrest at a specific stage of the cell cycle (Figure 4A). Surprisingly, despite complete cessation of proliferation for over 72 hr these cells remained viable, and a substantial fraction of the cells had a DNA content between 2N and 4N suggesting that some cells were unable to progress through S-phase. Furthermore, compared to cells proliferating in the presence of AKB, the non-proliferating population showed a subtle accumulation of cells with a DNA content less than 4N. An inability to generate sufficient nucleotides to support DNA synthesis can prevent progression through S-phase (Lunt et al., 2015). To determine if a deficiency in nucleotide synthesis contributes to the inability to proliferate in the absence of AKB, we quantified nucleotide pools in 143B CytB cells in the presence and absence of AKB using liquid chromatography mass spectrometry (LCMS). Because pyrimidine nucleotide pools are confounded by excess uridine supplemented in the media, we focused analysis on purine nucleotides. Compared to AKB replete cells, cells cultured without AKB had increased levels of the purine nucleotide inosine-5′-monophosphate (IMP) (Figure 4B). IMP is a precursor of both guanine-5′-monophosphate (GMP) and adenine-5′-monophosphate (AMP). However, despite an increase in IMP, both GMP and AMP levels were decreased in the absence of AKB (Figure 4B). To determine the functional significance of the purine nucleotide deficiency, we supplemented 143B CytB cells with exogenous adenine, guanine, and hypoxanthine. Using nucleotide salvage pathways, these nucleobases are converted to AMP, GMP, and IMP, respectively. Whereas hypoxanthine had no effect on proliferation and guanine supplementation was slightly toxic, adenine supplementation restored proliferation for one doubling, and alleviated the accumulation of cells with DNA content less than 4N (Figures 4C and S3A). These

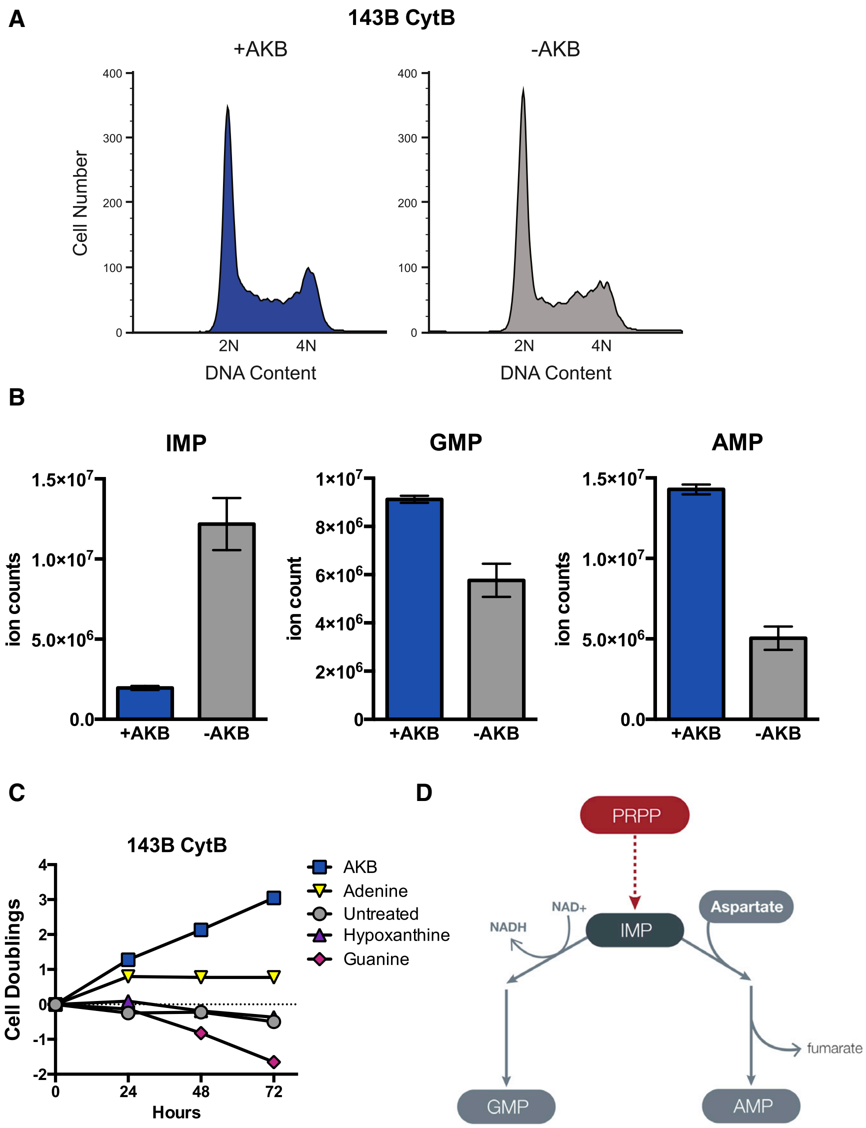

Figure 4. Electron Acceptor Insufficiency Affects Purine Nucleotide Levels

(A) Analysis of DNA content by propidium iodide staining and flow cytometry of 143B CytB cells cultured with our without AKB supplementation.

(B) LCMS quantification of purine nucleotide levels in 143B CytB cells cultured with or without AKB supplementation.

(C) Cell doublings were measured over time of 143B CytB cells cultured in unsupplemented media or media supplemented with AKB, adenine, hypoxanthine, or guanine.

(D) Schematic illustrating the use of IMP for GMP and AMP synthesis. Synthesis of GMP uses NAD+, whereas synthesis of AMP requires aspartate.

Values in (B) and (C) denote mean ± SEM, n = 3. See also Figure S3.

data suggest that loss of respiration impairs adenine nucleotide synthesis and that adenine nucleotide deficiency partially explains the inability of cells to proliferate in the absence of electron acceptors.

Both the AMP/IMP ratio and the GMP/IMP ratio dramatically decrease when AKB is withdrawn from cells cultured in the presence of this exogenous electron acceptor (Figure S3B). This decrease in the AMP/IMP and GMP/IMP ratios suggests an inability to convert IMP to either AMP or GMP. Conversion of IMP to GMP consumes an NAD+ by inosine 5′monophosphate dehydrogenase (IMPDH); thus, this reaction may be inhibited by decreased NAD+ availability (Figure 4D). In contrast, conversion of IMP to AMP does not directly require oxidation but instead consumes aspartate (Figure 4D). This suggests the possibility that decreased AMP production could be downstream of an aspartate deficiency. Consistent with this, SAICAR, a precursor to IMP that also requires aspartate for its synthesis is also depleted when AKB is withdrawn (Figure S3C). Importantly, an underlying aspartate deficiency could explain the transitory nature of adenine rescue; adenine can only restore proliferation to those cells in a phase of cell cycle where adenine is limiting and fails to compensate for other roles that aspartate might play in cell growth and division.

Aspartate Synthesis Is Inhibited by Electron Acceptor Insufficiency

For most cells in culture, carbon for de novo aspartate synthesis is supplied by anaplerotic glutamine (DeBerardinis et al., 2007; Hensley et al., 2013). Glutamine is converted to glutamate, which enters the TCA cycle upon conversion to alpha-ketoglutarate (AKG) by glutamate dehydrogenase (GDH) or transamination (Figure 5A). While GDH uses NAD+ as a co-substrate, the glutamate transaminases utilize alpha-ketoacids, such as pyruvate, as co-substrates. Regardless of which pathway produces AKG from glutamate, conversion of a carbon-nitrogen single bond to a carbon-oxygen double bond necessitates that an electron pair is transferred to an electron acceptor (Figure S4A).

Aspartate can be produced from AKG via both reductive and oxidative pathways. Reductive synthesis of aspartate by reductive carboxylation of AKG requires high levels of AKG (Fendt et al., 2013), and electron acceptors are needed to maintain increased AKG pools. In addition, NAD+ dependent oxidation of AKG is required to support reductive carboxylation of AKG, providing another mechanism by which electron acceptors are required for reductive aspartate synthesis (Mullen et al., 2014). Oxidative synthesis of aspartate from AKG requires three additional oxidation reactions requiring net transfer of two electron pairs, thus imposing a further requirement for additional electron acceptors to produce aspartate oxidatively from AKG (Figure 5A).

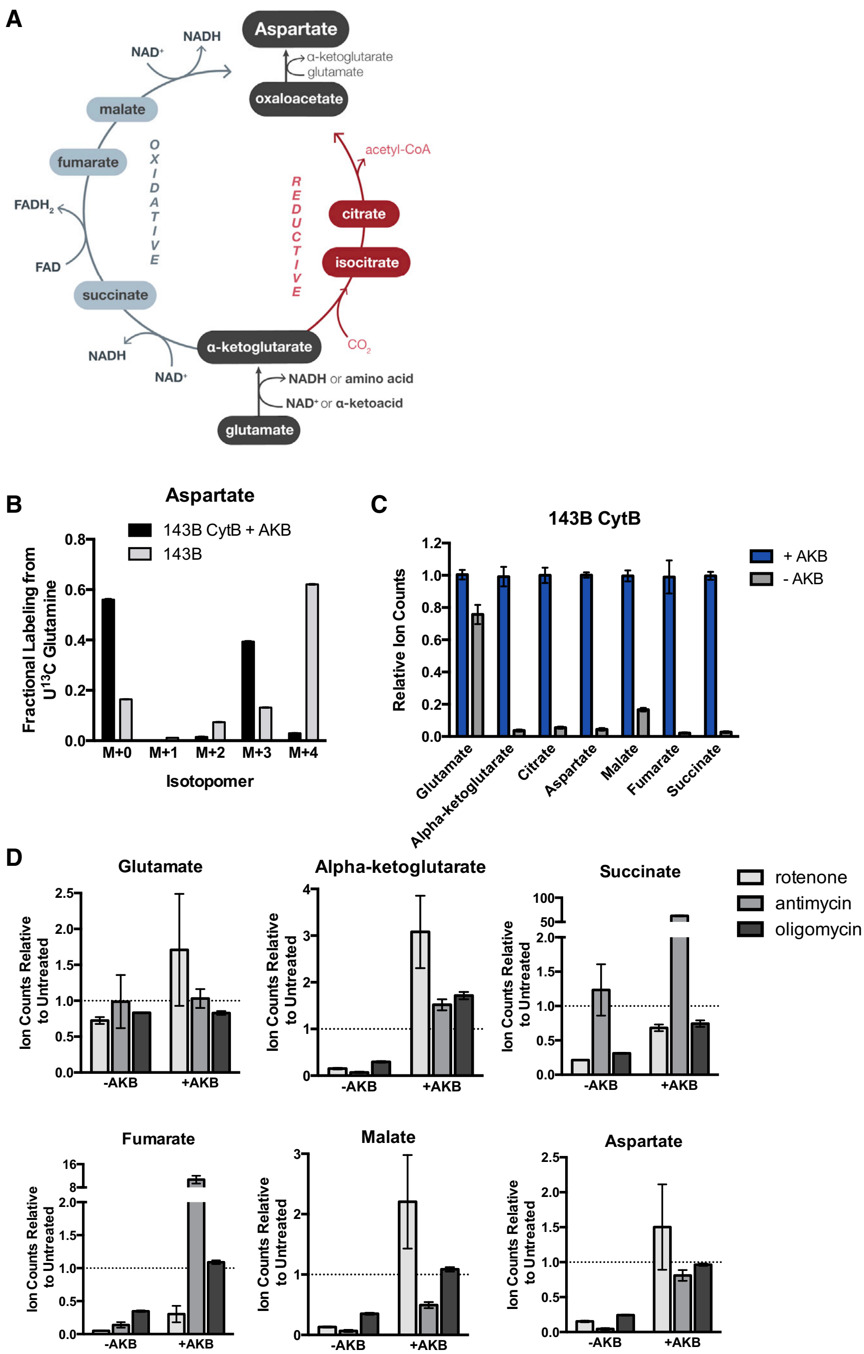

Figure 5. Electron Acceptor Insufficiency Suppresses TCA Metabolite and Aspartate Levels

(A) Schematic detailing the TCA-cycle reaction routes for the biosynthesis of aspartate from glutamine.

(B) Isotopomer distribution of aspartate from 143B CytB cells supplemented with AKB and 143B cells cultured in the presence of U-^{13}C Glutamine for 8 hr.

(C) GCMS quantification of TCA-cycle metabolites, glutamate, and aspartate from 143B CytB cells cultured with or without AKB.

(D) GCMS quantification of TCA metabolites, glutamate, and aspartate from 143B cells cultured with or without AKB in the presence or absence of the indicated mitochondrial inhibitors. Ion counts are relative to untreated 143B cells, which is denoted by the dashed gray line in each panel. Values denote mean ± SEM, n = 3. See also Figure S4.

Given that both aspartate synthesis pathways utilize electron acceptors, we reasoned that electron acceptor deficiency in respiration-inhibited cells could limit aspartate production and result in aspartate deficiency.

We used gas chromatography mass spectrometry (GCMS) to measure the electron acceptor dependency of glutamate, aspartate, and TCA-cycle metabolite levels in cells. In 143B CytB cells, which metabolize glutamine by reductive carboxylation (Figure 5B and S4B) (Mullen et al., 2012), glutamate levels are only modestly lower upon AKB withdrawal, whereas pool sizes of TCA-cycle metabolites are drastically decreased (Figure 5C). Aspartate was also dramatically decreased in these cells, supporting the hypothesis that aspartate limitation may explain the observed AMP/IMP imbalance in cells with electron acceptor insufficiency. In wild-type 143B cells, which normally produce aspartate by oxidative TCA-cycle metabolism (Figure 5B and S4B), treatment with the respiration inhibitors rotenone, antimycin, and oligomycin yielded similar results, with decreases in both TCA metabolites and aspartate but not glutamate (Figure 5D). In all cases, treatment with AKB restored aspartate to levels comparable to or higher than untreated cells. These data demonstrate that lack of available electron acceptors restricts aspartate biosynthesis.

Aspartate Restores Proliferation in Cells with Electron Acceptor Insufficiency

To determine if electron acceptor deficiency inhibits proliferation because of an effect on aspartate biosynthesis, we tested whether exogenous aspartate could replace the requirement for exogenous electron acceptors. Strikingly, in the absence of exogenous electron acceptors, supplementation with supra-physiological levels of aspartate was capable of supporting exponential growth of 143B CytB cells (Figure 6A). Given the decrease in other TCA-cycle intermediates observed following electron acceptor withdrawal, we also tested whether other TCA-cycle intermediates or their cell-permeable derivatives could restore proliferation of

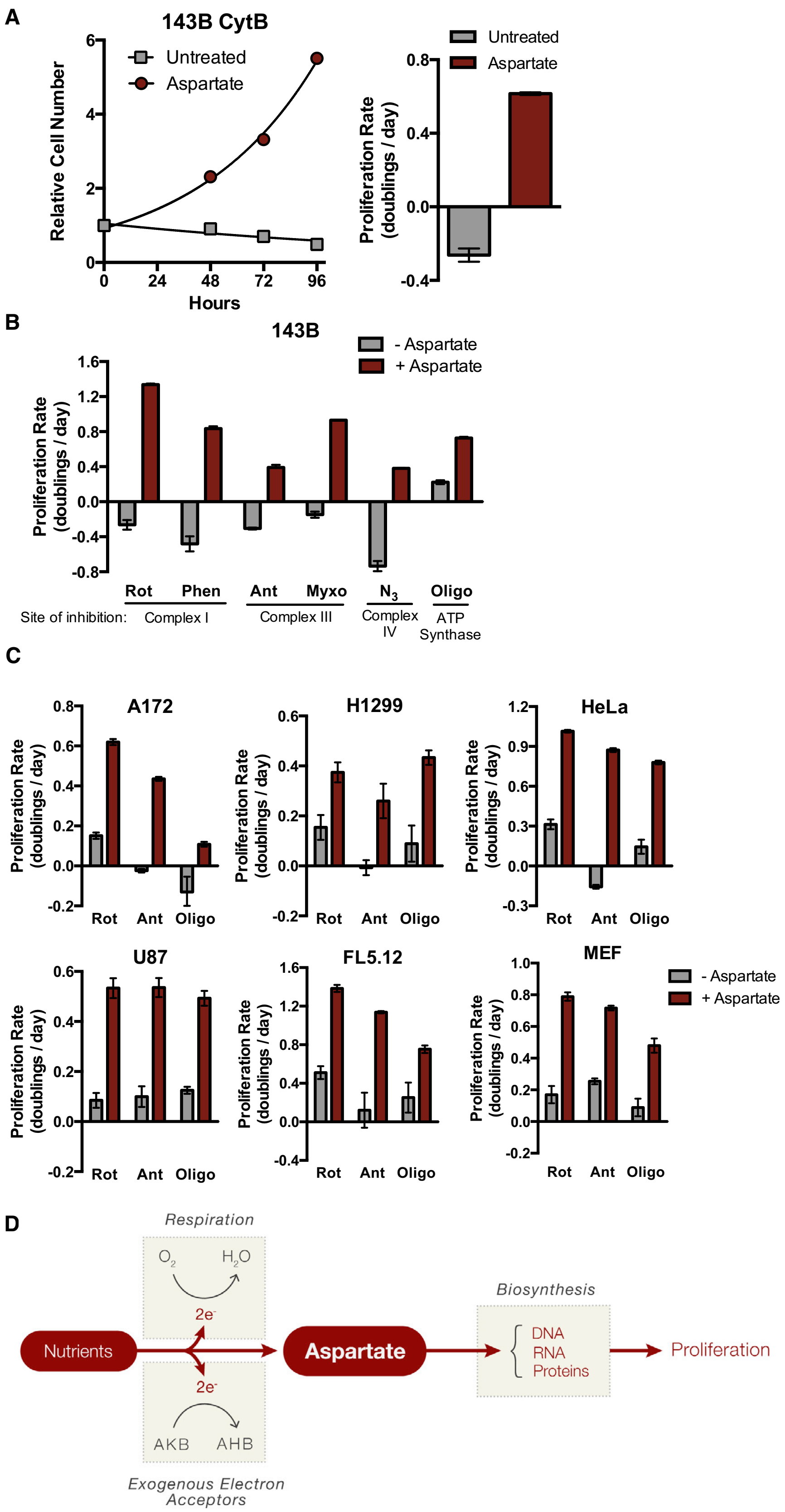

Figure 6. Aspartate is the Key Biosynthetic Precursor Provided by Respiration

(A) Proliferation rate of 143B CytB cells determined in the presence or absence of aspartate.

(B) The proliferation rate of 143B cells cultured with or without aspartate in the presence of the mitochondrial respiration inhibitors rotenone (Rot), phenformin (Phen), antimycin (Ant), myxothiazol (Myxo), azide (N_3), or oligomycin (Oligo).

(C) The proliferation rate of A172, H1299, HeLa, U87, FL5.12, and MEF cells cultured with or without aspartate in the presence of rotenone, antimycin, or oligomycin.

(D) Schematic detailing the role of respiration and exogenous electron acceptors in aspartate biosynthesis. The conversion of nutrients into aspartate requires the removal of electrons and therefore requires access to electron acceptors, which can be supplied by respiration (O_2) or exogenous electron acceptors such as AKB. Maintenance of aspartate pools supports nucleotide and protein biosynthesis. Values in all figure panels denote mean ± SEM, n = 3. See also Figure S5.

these cells. None were able to restore proliferation to a similar degree as aspartate (Figures S5A and S5B). Respiration-competent 143B WT cybrid cells proliferated at similar rates in the presence or absence of aspartate (Figure S5C). Importantly, aspartate does not function as an exogenous electron acceptor as it neither increases mitochondrial oxygen consumption, nor does it alter the NAD+/NADH ratio in 143B CytB cells (Figures S5D and S5E). These data imply that aspartate is not an electron acceptor but rather is itself the biosynthetic demand that becomes limiting for proliferation in electron acceptor deficient cells.

Measurement of purine nucleotides shows that in 143B CytB cells aspartate addition relieves IMP accumulation and restores AMP pools (Figure S5F). This is consistent with the hypothesis that under electron acceptor deficiency, aspartate is limiting for adenine nucleotide synthesis. Aspartate treatment also restored SAICAR levels, another intermediate limited by aspartate availability (Figure S5G). Interestingly, GMP levels are not restored by aspartate treatment, consistent with the conversion of IMP to GMP being dependent on NAD+, which is not restored by aspartate (Figures S5E and S5F). Indeed, GMP levels were lower in aspartate-treated cells, likely a result of decreased IMP availability.

To determine whether aspartate is sufficient to restore proliferation in wild-type cells where respiration is inhibited, wild-type 143B cells were treated with various respiration inhibitors with or without aspartate supplementation. Aspartate restored proliferation of cells treated with all ETC inhibitors (Figure 6B). Aspartate addition also rescued ETC inhibitor-induced proliferation decreases in all other cell lines tested (Figure 6C).

Taken together, these data support a model where a major metabolic requirement for proliferating cells fulfilled by respiration is providing access to electron acceptors in the form of oxygen. This access to electron acceptors is required to support de novo aspartate biosynthesis and in the absence of mitochondrial respiration, the demand for oxygen can be met through supplementation of other electron acceptors such as pyruvate or AKB. Alternatively, if the demand for aspartate can be met exogenously, electron acceptors become dispensable for proliferation. Surprisingly, this implies that the major function of respiration in proliferating cells is to support aspartate synthesis (Figure 6D).

DISCUSSION

In this study we examine the role of mitochondrial respiration in proliferative metabolism. Whereas respiration is primarily an ATP-producing catabolic process in non-proliferating cells, in proliferating cells respiration serves a crucial anabolic role by providing access to electron acceptors to support aspartate synthesis. Furthermore, mitochondrial ATP production appears dispensable in proliferating cells with access to sufficient glucose. Proliferating cells have different metabolic requirements than non-proliferating cells (Lunt and Vander Heiden, 2011); yet in both cases, the components of the metabolic network are largely the same (Hu et al., 2013). During proliferation these same network components must take on distinct roles to balance the contrasting anabolic and catabolic needs of the cell. While respiration likely supports ATP production in addition to aspartate biosynthesis in many contexts, our finding that respiration is specifically required for aspartate biosynthesis in proliferating cells highlights a distinct anabolic role for respiration.

All cells must perform thermodynamically unfavorable processes. One way to accomplish this is to harness the free-energy of nutrient oxidation. The source of electron donors for oxidation varies widely across species from inorganic material for chemolithotrophic bacteria to reduced carbon for most heterotrophs including mammalian cells. In all cases, nutrient oxidation requires net transfer of electrons to a terminal electron acceptor. In mammalian cells, substrates for nutrient oxidation include carbohydrates, lipids, and amino acids. Various metabolic pathways, including the TCA cycle, are employed for nutrient oxidation with electrons transferred initially to electron accepting cofactors such as NAD+ or FAD. These reactions yield NADH or $FADH_2$, respectively, and result in production of intermediates with more oxidized carbon. The electrons from the reduced cofactors are transferred to the ETC, which uses O_2 as a terminal electron acceptor to produce water and facilitate ATP production. Importantly, ATP production through this process intimately couples the oxidation of carbon substrates to O_2 consumption.

In contexts where mammalian cells cannot utilize O_2 as a terminal electron acceptor, cells are unable to regenerate oxidized cofactors via the ETC. Cells can ferment pyruvate to lactate to regenerate NAD+; however, because the glyceraldehyde 3-phosphate dehydrogenase (GAPDH) step of glycolysis consumes NAD+, use of glucose-derived pyruvate for lactate fermentation does not net yield NAD+. Thus, in the absence of access to exogenous electron acceptors, in order to maintain redox balance and sustain glycolytic ATP production most glucose carbon metabolized via glycolysis past the GAPDH step must be excreted as lactate. While fermentation can produce sufficient ATP for proliferation, it is a redox neutral pathway. In the absence of exogenous electron acceptors cells cannot net synthesize molecules that are more oxidized than the nutrients consumed. Thus, losing oxygen as an electron acceptor results in the inability to net remove electrons from consumed carbon substrates.

Proliferating cells must duplicate all cell components, some of which are more oxidized than the nutrients consumed. This suggests that net removal of electrons from carbon is an intrinsic anabolic requirement to support production of oxidized molecules, such as nucleotides, for biomass accumulation. The need to oxidize nutrients to generate biomass may result in electron acceptor insufficiency and limit proliferation even in the presence of oxygen. Notably, the NAD+/NADH ratio in normoxic cancer cells is more reduced than previously assumed (Hung et al., 2011; Zhao et al., 2015), consistent with oxidation capacity being constrained. Because the NAD+/NADH ratio and the pyruvate/lactate ratio are tightly coupled in cells (Williamson et al., 1967), a low NAD+/NADH ratio is expected to drive increased pyruvate to lactate conversion. This raises the possibility that the Warburg effect is a reflection of electron acceptor insufficiency.

Here, we find that electron acceptors are most limiting for de novo aspartate synthesis. While cells in culture are exposed to atmospheric oxygen, oxygen availability in animal tissues is much lower (Bertout et al., 2008). Therefore, it may be advantageous for cells to utilize less oxidative pathways when electron acceptors become more limiting. The need for electron acceptors is decreased when metabolic pathways that fix CO_2 are used for de novo aspartate synthesis. For instance, pyruvate carboxylation produces oxaloacetate that can be transaminated to form aspartate. Alternatively, reductive AKG carboxylation can generate isocitrate, which can be isomerized to citrate, cleaved to form oxaloacetate, and transaminated to produce aspartate. In both cases, fully oxidized carbon is incorporated to produce aspartate without directly requiring net removal of electrons. However, pyruvate and AKG are themselves oxidized relative to the major nutrients glucose and glutamine, imposing a need for electron acceptors to produce these carboxylation pathway substrates. Furthermore, the ability to maintain increased levels of pyruvate or AKG to support pyruvate carboxylation or reductive isocitrate dehydrogenase metabolism is compromised in electron acceptor deficient cells as illustrated by the dramatic fall in AKG levels when respiration is inhibited (Figures 5B and 5C). Therefore, regardless of the biosynthesis pathway used, electron acceptor insufficiency will limit aspartate synthesis.

Beyond its role as an amino acid in proteins, aspartate is required for conversion of IMP to AMP in de novo purine synthesis and provides the carbon backbone for de novo pyrimidine synthesis. Thus, aspartate deficiency will impair protein, purine nucleotide, and pyrimidine nucleotide synthesis. Notably, aspartate is inefficiently transported into most mammalian cells (Birsoy et al., 2015, this issue), with supra-physiological concentrations required to restore growth in electron acceptor deficient cells. The concentration of aspartate in blood is around 10 μM, among the lowest levels of all circulating amino acids (Mayers and Vander Heiden, 2015). Additionally, aspartate aminotransferase is among the most abundant enzymes in the liver, suggesting that circulating aspartate may be actively maintained at low levels. Given the critical roles of aspartate in biosynthesis and the challenges associated with obtaining aspartate from the blood, access to electron acceptors for aspartate synthesis may be a requirement for proliferation in many tumors. Consistent with this idea, pharmacologic inhibition of ETC activity inhibits tumor growth in several cancer models (Shackelford et al., 2013; Wheaton et al., 2014; Zhang et al., 2014). Additionally, while ρ^0 cells are unable to form xenografts, reconstituting mtDNA in these cells restores tumorigenicity (Hayashi et al., 1992). This requirement for mtDNA appears so stringent that, in one study, injected ρ^0 cells formed tumors only after acquiring mtDNA from the host (Tan et al., 2015). While ρ^0 cells are also expected to be pyrimidine-limited due to loss of DHODH activity, genetic loss of complex I, which blocks respiration but not DHODH, also impairs tumorigenesis (Park et al., 2009).

Beyond loss of aspartate biosynthesis, we find loss of ETC activity affects the NAD+/NADH ratio. This redox change will also influence other pathways. For example, NAD+ is integral to sirtuin and PARP activity, and thus, loss of ETC activity may perturb signaling pathways (Cantó and Auwerx, 2011). Additionally, ETC activity impacts apoptosis (Newmeyer and Ferguson-Miller, 2003; Wallace, 2012), processes that depend on the mitochondrial membrane potential (Chen et al., 2014; Geissler et al., 2000), and reactive oxygen species (ROS) levels in cells (Schieber and Chandel, 2014). Mutations in ETC components resulting in partial inhibition of respiration may even be advantageous for proliferation in certain contexts by increasing ROS production (Petros et al., 2005). Nevertheless, exogenous aspartate addition is sufficient to restore proliferation of cells that otherwise stop proliferating or die when ETC activity is impaired. Thus, a primary role for mitochondrial respiration in cell proliferation must be to provide access to electron acceptors in support of aspartate synthesis.

EXPERIMENTAL PROCEDURES

Cell Culture

143B, A172, H1299, HeLa, U87, 143B cybrid cell lines (WT Cybrid and CytB), FL5.12, and immortalized MEF cells were cultured in Dulbecco's Modified Eagle's Medium (DMEM) (GIBCO) supplemented with 10% fetal bovine serum and penicillin-streptomycin. FL5.12 cells were supplemented with 5 μg/ml recombinant mouse IL-3 (R&D Systems), and 143B cybrid cells were supplemented 0.1 mg/ml uridine. All cells were incubated at 37°C with 5% CO_2.

Proliferation Rates

Cell were plated onto replicate 6-well dishes (Corning), with initial seeding density of 20,000 cells per well for 143B, A172, H1299, HeLa, 143B WT Cybrid, FL5.12, and MEFs and 30,000 cells for 143B CytB and U87 cells. After overnight incubation for cells to adhere, 6 wells were counted to determine initial count at time of treatment. Cells were washed twice in phosphate buffered saline (PBS) and 4 ml of treatment media was added. Final cell counts were measured 4 days after treatment, and proliferation rate was calculated. See Supplemental Experimental Procedures for detailed protocol. Concentrations of all metabolites and compounds added to culture media for each cell line are included as a table in Supplemental Experimental Procedures (Table S1).

Mitochondrial Oxygen Consumption

Oxygen consumption rates were determined using a Seahorse Bioscience Extracellular Flux Analyzer (XF24). See Supplemental Experimental Procedures for detailed protocol.

Purine Nucleotide Metabolite Extraction and LCMS Analysis

Cells were treated as indicated for 15 hr and polar metabolites were extracted. A Dionex UltiMate 3000 ultra-high performance liquid chromatography system connected to a Q Exactive benchtop Orbitrap mass spectrometer, equipped with an Ion Max source and a HESI II probe (Thermo Fisher Scientific), was used to quantify metabolites. See Supplemental Experimental Procedures for detailed extraction and LCMS conditions.

Amino Acid and TCA-Cycle Metabolite Extraction and GCMS Analysis

Cells were seeded at 400,000 cells/well in 6-well dishes overnight. The following day cells were washed twice in PBS and media was changed to media containing the indicated treatments. After 8 hr, polar metabolites were extracted using 80% methanol in water with 1 μg norvaline standard added per sample. Soluble content was dried under nitrogen gas. Polar samples were derivatized and measured as previously detailed (Lewis et al., 2014). Relative metabolite abundances were determined by integrating ion peak area (Metran) and normalized to norvaline internal extraction standard.

Cell-Cycle Distribution Measurements

Cells were incubated with or without AKB or 100 μM adenine as indicated for 78 hr before being washed with PBS, trypsinized, pelleted, and resuspended in 500 μl PBS. Cells were fixed by adding 4.5 ml 70% ethanol and incubated at 4°C overnight. Cells were then pelleted and resuspended in 1 ml PBS + 0.1% (v/v) Triton X-100. RNase A and propidium iodide (PI) were added to 0.2 mg/ml and 20 μg/ml, respectively. Samples were incubated at 37°C for

15 min and filtered into a flow cytometry tube. DNA content was measured by flow cytometry (BD FACS Canto II) and analyzed (FACS Diva Software).

Measurement of NAD+/NADH

Cells were plated in the same manner as proliferation assays and treated as indicated prior to preparation of cell extracts 6 hr after treatment. NAD+/NADH was measured using a modified version of the manufacturer instructions supplied with the NAD/NADH Glo Assay (Promega). See Supplemental Experimental Procedures for a detailed protocol.

SUPPLEMENTAL INFORMATION

Supplemental Information includes Supplemental Experimental Procedures, five figures, and one table and can be found with this article online at http://dx.doi.org/10.1016/j.cell.2015.07.017.

AUTHOR CONTRIBUTIONS

L.B.S. and D.Y.G. performed experiments to determine proliferation rates, NAD+/NADH, metabolite quantifications, and oxygen consumption rates. A.M.H. performed cell-cycle analysis experiments. L.N.B. performed proliferation rate experiments. E.F. performed LCMS quantification. L.B.S., D.Y.G., and M.G.V.H. designed the study and wrote the manuscript.

ACKNOWLEDGMENTS

This work was supported by the Burroughs Wellcome Fund and the NIH (P30CA1405141, GG006413, and R01 CA168653) to M.G.V.H., a postdoctoral fellowship, PF-15-096-01-TBE from the American Cancer Society to L.B.S., NIH (T32 GM007753) to D.Y.G., HHMI International Student Research fellowship and the Vertex Scholars Program to A.M.H., and Alex's Lemonade Stand Undergraduate Research Fellowship to L.N.B., We thank Alena Heath for graphic design and members of the Vander Heiden lab for thoughtful discussion. We also thank C. Moraes, I.F.M. de Coo, and Navdeep Chandel for the 143B CytB and 143B WT cybrid cell lines. M.G.V.H. is a consultant and SAB member for Agios Pharmaceuticals which seeks to target metabolism for cancer therapy.

Received: June 8, 2015
Revised: July 6, 2015
Accepted: July 8, 2015
Published: July 30, 2015

REFERENCES

Bertout, J.A., Patel, S.A., and Simon, M.C. (2008). The impact of O2 availability on human cancer. Nat. Rev. Cancer *8*, 967–975.

Birsoy, K., Wang, T., Chen, W., Freinkman, E., Abu-Remaileh, M., and Sabatini, D.M. (2015). An Essential Role of the Mitochondrial Electron Transport Chain in Cell Proliferation Is to Enable Aspartate Synthesis. Cell *162*, this issue, 540–551.

Brand, M.D., and Nicholls, D.G. (2011). Assessing mitochondrial dysfunction in cells. Biochem. J. *435*, 297–312.

Cantó, C., and Auwerx, J. (2011). NAD+ as a signaling molecule modulating metabolism. Cold Spring Harb. Symp. Quant. Biol. *76*, 291–298.

Chen, W.W., Birsoy, K., Mihaylova, M.M., Snitkin, H., Stasinski, I., Yucel, B., Bayraktar, E.C., Carette, J.E., Clish, C.B., Brummelkamp, T.R., et al. (2014). Inhibition of ATPIF1 ameliorates severe mitochondrial respiratory chain dysfunction in mammalian cells. Cell Rep. *7*, 27–34.

DeBerardinis, R.J., Mancuso, A., Daikhin, E., Nissim, I., Yudkoff, M., Wehrli, S., and Thompson, C.B. (2007). Beyond aerobic glycolysis: transformed cells can engage in glutamine metabolism that exceeds the requirement for protein and nucleotide synthesis. Proc. Natl. Acad. Sci. USA *104*, 19345–19350.

Fan, J., Kamphorst, J.J., Mathew, R., Chung, M.K., White, E., Shlomi, T., and Rabinowitz, J.D. (2013). Glutamine-driven oxidative phosphorylation is a major ATP source in transformed mammalian cells in both normoxia and hypoxia. Mol. Syst. Biol. *9*, 712.

Fendt, S.M., Bell, E.L., Keibler, M.A., Olenchock, B.A., Mayers, J.R., Wasylenko, T.M., Vokes, N.I., Guarente, L., Vander Heiden, M.G., and Stephanopoulos, G. (2013). Reductive glutamine metabolism is a function of the α-ketoglutarate to citrate ratio in cells. Nat. Commun. *4*, 2236.

Geissler, A., Krimmer, T., Bömer, U., Guiard, B., Rassow, J., and Pfanner, N. (2000). Membrane potential-driven protein import into mitochondria. The sorting sequence of cytochrome b(2) modulates the deltapsi-dependence of translocation of the matrix-targeting sequence. Mol. Biol. Cell *11*, 3977–3991.

Gottlieb, E., and Tomlinson, I.P. (2005). Mitochondrial tumour suppressors: a genetic and biochemical update. Nat. Rev. Cancer *5*, 857–866.

Grégoire, M., Morais, R., Quilliam, M.A., and Gravel, D. (1984). On auxotrophy for pyrimidines of respiration-deficient chick embryo cells. Eur. J. Biochem. *142*, 49–55.

Harms, M., and Seale, P. (2013). Brown and beige fat: development, function and therapeutic potential. Nat. Med. *19*, 1252–1263.

Harris, M. (1980). Pyruvate blocks expression of sensitivity to antimycin A and chloramphenicol. Somatic Cell Genet. *6*, 699–708.

Hayashi, J., Takemitsu, M., and Nonaka, I. (1992). Recovery of the missing tumorigenicity in mitochondrial DNA-less HeLa cells by introduction of mitochondrial DNA from normal human cells. Somat. Cell Mol. Genet. *18*, 123–129.

Hensley, C.T., Wasti, A.T., and DeBerardinis, R.J. (2013). Glutamine and cancer: cell biology, physiology, and clinical opportunities. J. Clin. Invest. *123*, 3678–3684.

Howell, N., and Sager, R. (1979). Cytoplasmic genetics of mammalian cells: conditional sensitivity to mitochondrial inhibitors and isolation of new mutant phenotypes. Somatic Cell Genet. *5*, 833–845.

Hu, J., Locasale, J.W., Bielas, J.H., O'Sullivan, J., Sheahan, K., Cantley, L.C., Vander Heiden, M.G., and Vitkup, D. (2013). Heterogeneity of tumor-induced gene expression changes in the human metabolic network. Nat. Biotechnol. *31*, 522–529.

Hung, Y.P., Albeck, J.G., Tantama, M., and Yellen, G. (2011). Imaging cytosolic NADH-NAD(+) redox state with a genetically encoded fluorescent biosensor. Cell Metab. *14*, 545–554.

King, M.P., and Attardi, G. (1989). Human cells lacking mtDNA: repopulation with exogenous mitochondria by complementation. Science *246*, 500–503.

King, M.P., and Attardi, G. (1996). Isolation of human cell lines lacking mitochondrial DNA. Methods Enzymol. *264*, 304–313.

Koppenol, W.H., Bounds, P.L., and Dang, C.V. (2011). Otto Warburg's contributions to current concepts of cancer metabolism. Nat. Rev. Cancer *11*, 325–337.

Kovacević, Z. (1971). The pathway of glutamine and glutamate oxidation in isolated mitochondria from mammalian cells. Biochem. J. *125*, 757–763.

Kroll, W., Löffler, M., and Schneider, F. (1983). Energy parameters, macromolecular synthesis and cell cycle progression of in vitro grown Ehrlich ascites tumor cells after inhibition of oxidative ATP synthesis by oligomycin. Z. Naturforsch., C, Biosci. *38*, 604–612.

Lewis, C.A., Parker, S.J., Fiske, B.P., McCloskey, D., Gui, D.Y., Green, C.R., Vokes, N.I., Feist, A.M., Vander Heiden, M.G., and Metallo, C.M. (2014). Tracing compartmentalized NADPH metabolism in the cytosol and mitochondria of mammalian cells. Mol. Cell *55*, 253–263.

Löffer, M., and Schneider, F. (1982). Further characterization of the growth inhibitory effect of rotenone on in vitro cultured Ehrlich ascites tumour cells. Mol. Cell. Biochem. *48*, 77–90.

Lunt, S.Y., and Vander Heiden, M.G. (2011). Aerobic glycolysis: meeting the metabolic requirements of cell proliferation. Annu. Rev. Cell Dev. Biol. *27*, 441–464.

Lunt, S.Y., Muralidhar, V., Hosios, A.M., Israelsen, W.J., Gui, D.Y., Newhouse, L., Ogrodzinski, M., Hecht, V., Xu, K., Acevedo, P.N., et al. (2015). Pyruvate kinase isoform expression alters nucleotide synthesis to impact cell proliferation. Mol. Cell *57*, 95–107.

Mayers, J.R., and Vander Heiden, M.G. (2015). Famine versus feast: understanding the metabolism of tumors in vivo. Trends Biochem. Sci. *40*, 130–140.

Mitchell, P. (1961). Coupling of phosphorylation to electron and hydrogen transfer by a chemi-osmotic type of mechanism. Nature *191*, 144–148.

Morais, R., Zinkewich-Péotti, K., Parent, M., Wang, H., Babai, F., and Zollinger, M. (1994). Tumor-forming ability in athymic nude mice of human cell lines devoid of mitochondrial DNA. Cancer Res. *54*, 3889–3896.

Mullen, A.R., Wheaton, W.W., Jin, E.S., Chen, P.H., Sullivan, L.B., Cheng, T., Yang, Y., Linehan, W.M., Chandel, N.S., and DeBerardinis, R.J. (2012). Reductive carboxylation supports growth in tumour cells with defective mitochondria. Nature *481*, 385–388.

Mullen, A.R., Hu, Z., Shi, X., Jiang, L., Boroughs, L.K., Kovacs, Z., Boriack, R., Rakheja, D., Sullivan, L.B., Linehan, W.M., et al. (2014). Oxidation of alpha-ketoglutarate is required for reductive carboxylation in cancer cells with mitochondrial defects. Cell Rep. *7*, 1679–1690.

Newmeyer, D.D., and Ferguson-Miller, S. (2003). Mitochondria: releasing power for life and unleashing the machineries of death. Cell *112*, 481–490.

Park, J.S., Sharma, L.K., Li, H., Xiang, R., Holstein, D., Wu, J., Lechleiter, J., Naylor, S.L., Deng, J.J., Lu, J., and Bai, Y. (2009). A heteroplasmic, not homoplasmic, mitochondrial DNA mutation promotes tumorigenesis via alteration in reactive oxygen species generation and apoptosis. Hum. Mol. Genet. *18*, 1578–1589.

Petros, J.A., Baumann, A.K., Ruiz-Pesini, E., Amin, M.B., Sun, C.Q., Hall, J., Lim, S., Issa, M.M., Flanders, W.D., Hosseini, S.H., et al. (2005). mtDNA mutations increase tumorigenicity in prostate cancer. Proc. Natl. Acad. Sci. USA *102*, 719–724.

Rana, M., de Coo, I., Diaz, F., Smeets, H., and Moraes, C.T. (2000). An out-of-frame cytochrome b gene deletion from a patient with parkinsonism is associated with impaired complex III assembly and an increase in free radical production. Ann. Neurol. *48*, 774–781.

Schieber, M., and Chandel, N.S. (2014). ROS function in redox signaling and oxidative stress. Curr. Biol. *24*, R453–R462.

Schleyer, M., Schmidt, B., and Neupert, W. (1982). Requirement of a membrane potential for the posttranslational transfer of proteins into mitochondria. Eur. J. Biochem. *125*, 109–116.

Shackelford, D.B., Abt, E., Gerken, L., Vasquez, D.S., Seki, A., Leblanc, M., Wei, L., Fishbein, M.C., Czernin, J., Mischel, P.S., and Shaw, R.J. (2013). LKB1 inactivation dictates therapeutic response of non-small cell lung cancer to the metabolism drug phenformin. Cancer Cell *23*, 143–158.

Tan, A.S., Baty, J.W., Dong, L.F., Bezawork-Geleta, A., Endaya, B., Goodwin, J., Bajzikova, M., Kovarova, J., Peterka, M., Yan, B., et al. (2015). Mitochondrial genome acquisition restores respiratory function and tumorigenic potential of cancer cells without mitochondrial DNA. Cell Metab. *21*, 81–94.

van den Bogert, C., Spelbrink, J.N., and Dekker, H.L. (1992). Relationship between culture conditions and the dependency on mitochondrial function of mammalian cell proliferation. J. Cell. Physiol. *152*, 632–638.

Wallace, D.C. (2012). Mitochondria and cancer. Nat. Rev. Cancer *12*, 685–698.

Warburg, O. (1956). On the origin of cancer cells. Science *123*, 309–314.

Warburg, O., Posener, K., and Negelein, E. (1924). On the metabolism of carcinoma cells. Biochem. Z. *152*, 309–344.

Weinberg, F., Hamanaka, R., Wheaton, W.W., Weinberg, S., Joseph, J., Lopez, M., Kalyanaraman, B., Mutlu, G.M., Budinger, G.R., and Chandel, N.S. (2010). Mitochondrial metabolism and ROS generation are essential for Kras-mediated tumorigenicity. Proc. Natl. Acad. Sci. USA *107*, 8788–8793.

Weinhouse, S. (1956). On respiratory impairment in cancer cells. Science *124*, 267–269.

Wheaton, W.W., Weinberg, S.E., Hamanaka, R.B., Soberanes, S., Sullivan, L.B., Anso, E., Glasauer, A., Dufour, E., Mutlu, G.M., Budigner, G.S., and Chandel, N.S. (2014). Metformin inhibits mitochondrial complex I of cancer cells to reduce tumorigenesis. eLife *3*, e02242.

Williamson, D.H., Lund, P., and Krebs, H.A. (1967). The redox state of free nicotinamide-adenine dinucleotide in the cytoplasm and mitochondria of rat liver. Biochem. J. *103*, 514–527.

Zhang, X., Fryknäs, M., Hernlund, E., Fayad, W., De Milito, A., Olofsson, M.H., Gogvadze, V., Dang, L., Påhlman, S., Schughart, L.A., et al. (2014). Induction of mitochondrial dysfunction as a strategy for targeting tumour cells in metabolically compromised microenvironments. Nat. Commun. *5*, 3295.

Zhao, Y., Hu, Q., Cheng, F., Su, N., Wang, A., Zou, Y., Hu, H., Chen, X., Zhou, H.M., Huang, X., et al. (2015). SoNar, a Highly Responsive NAD+/NADH Sensor, Allows High-Throughput Metabolic Screening of Anti-tumor Agents. Cell Metab. *21*, 777–789.

Zielke, H.R., Zielke, C.L., and Ozand, P.T. (1984). Glutamine: a major energy source for cultured mammalian cells. Fed. Proc. *43*, 121–125.

Zu, X.L., and Guppy, M. (2004). Cancer metabolism: facts, fantasy, and fiction. Biochem. Biophys. Res. Commun. *313*, 459–465.

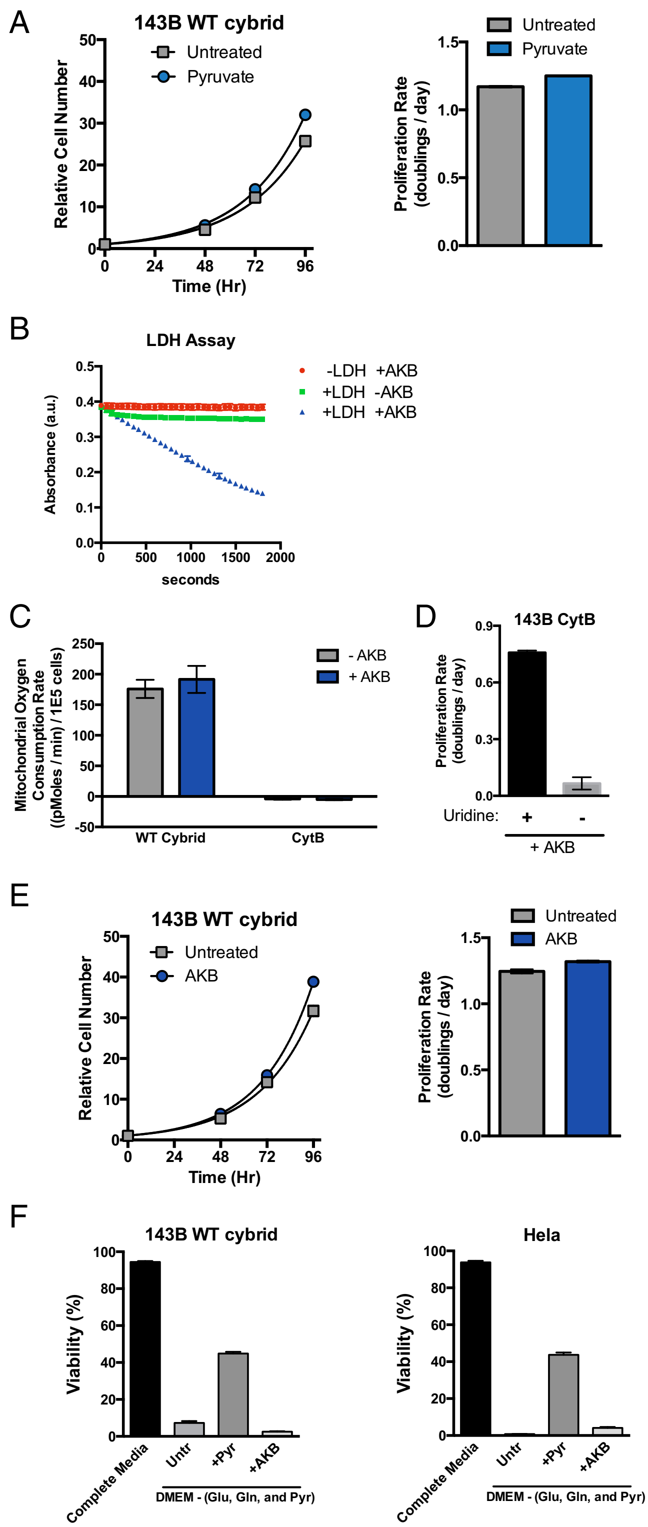

Figure S1. AKB Can Function as a Substrate for LDH and Does Not Restore Oxygen Consumption or Replace Uridine Auxotrophy in Respiration Incompetent Cells, Related to Figure 1

(A) Proliferation of 143B WT cybrid cells in the presence or absence of pyruvate. (B) The ability of lactate dehydrogenase (LDH) to use AKB as a substrate was assessed by changes in NADH absorbance (at 340 nm) in the presence or absence of AKB and LDH as indicated. (C) Mitochondrial oxygen consumption rate of 143B WT cybrid and 143B CytB cells in the presence or absence of AKB. (D) Proliferation rate of 143B CytB cells cultured in the presence of

(legend continued on next page)

AKB was determined with or without uridine supplementation. (E) Proliferation of 143B WT cybrid cells was determined in the presence or absence of AKB. (F) Viability was determined by propidium iodide exclusion for 143B WT cybrid and HeLa cells cultured in complete DMEM or DMEM without glucose, glutamine, or pyruvate, in the presence or absence of pyruvate or AKB supplementation as indicated. Values in all figures denote mean ± SEM, n = 3 (A, B, D–F), n = 5 (C).

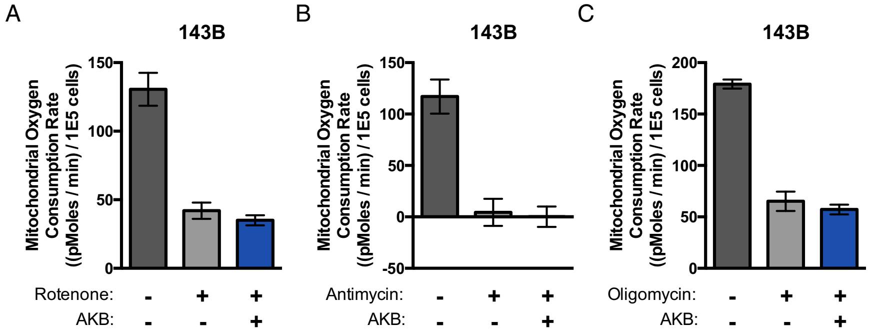

Figure S2. Mitochondrial Oxygen Consumption Is Inhibited by Respiration Inhibitors and Is Not Restored by AKB, Related to Figure 2
(A–C) Mitochondrial oxygen consumption rate of untreated 143B cells or 143B cells treated with rotenone (A), antimycin (B), or oligomycin (C), with or without AKB treatment. Values in all figures denote mean ± SEM, n = 5.

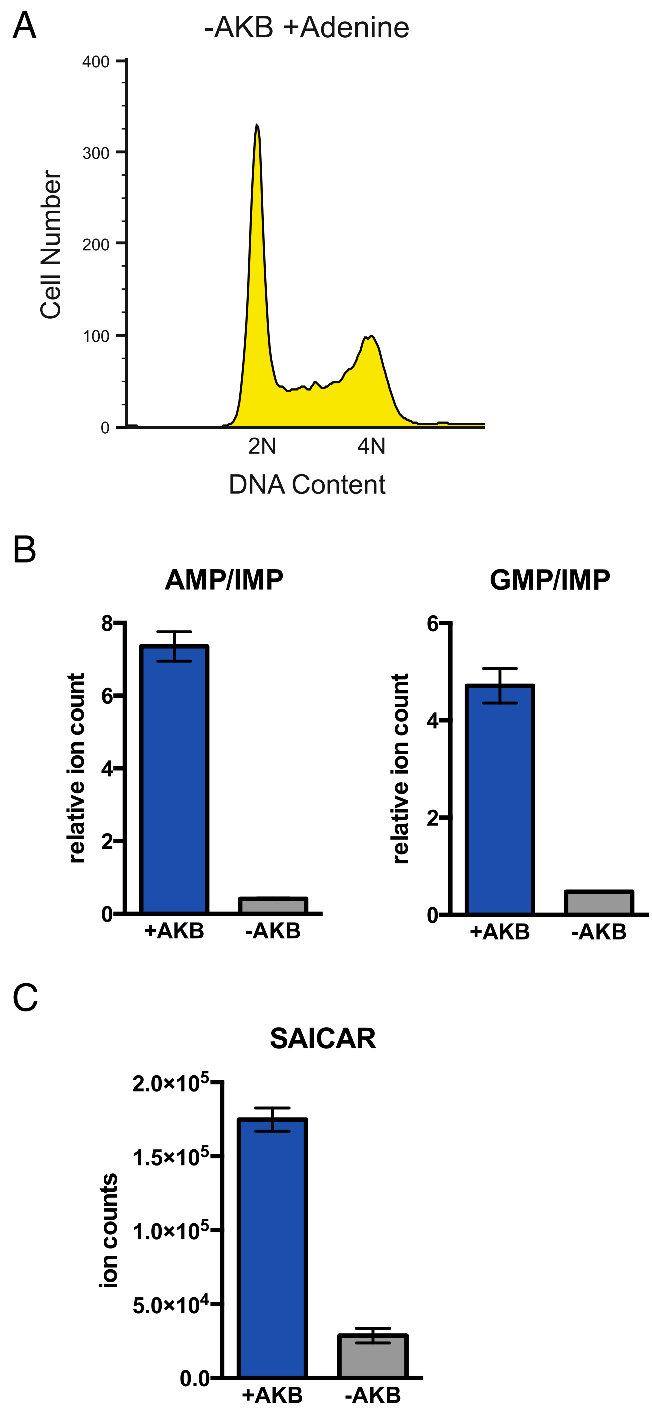

Figure S3. The Effect of Adenine on DNA Content and the Effect of AKB on Purine Nucleotide Ratios, Related to Figure 4

(A) Analysis of DNA content by propidium iodide staining and flow cytometry of 143B CytB cells without AKB supplementation and with adenine supplementation. (B) Relative ion count ratios of AMP to IMP and GMP to IMP in 143B CytB cells with or without AKB supplementation. (C) LCMS quantification of SAICAR levels in 143B CytB cells cultured with or without AKB supplementation. Values denote mean ± SEM, n = 3.

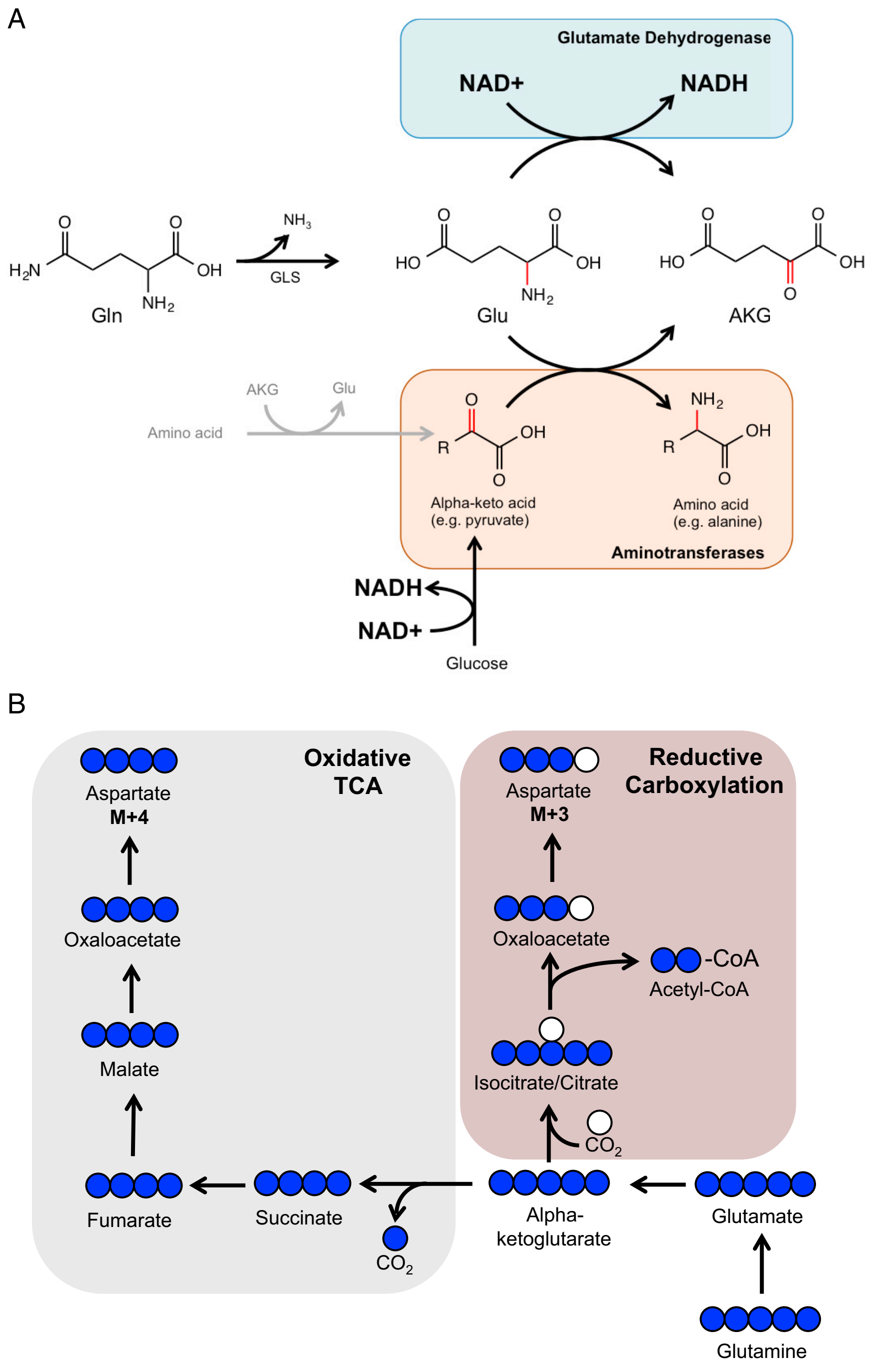

Figure S4. Aspartate is Derived from Glutamine by Reductive Carboxylation in 143B CytB Cells and Oxidative TCA Metabolism in 143B Cells, Related to Figure 5

(A) Schematic detailing the pathways used to produce alpha-ketoglutarate from glutamine. Abbreviations: Gln, glutamine; Glu, glutamic acid; AKG, alpha-ketoglutaric acid. (B) Schematic showing expected aspartate labeling patterns if synthesized from glutamine using oxidative TCA metabolism or reductive carboxylation as indicated.

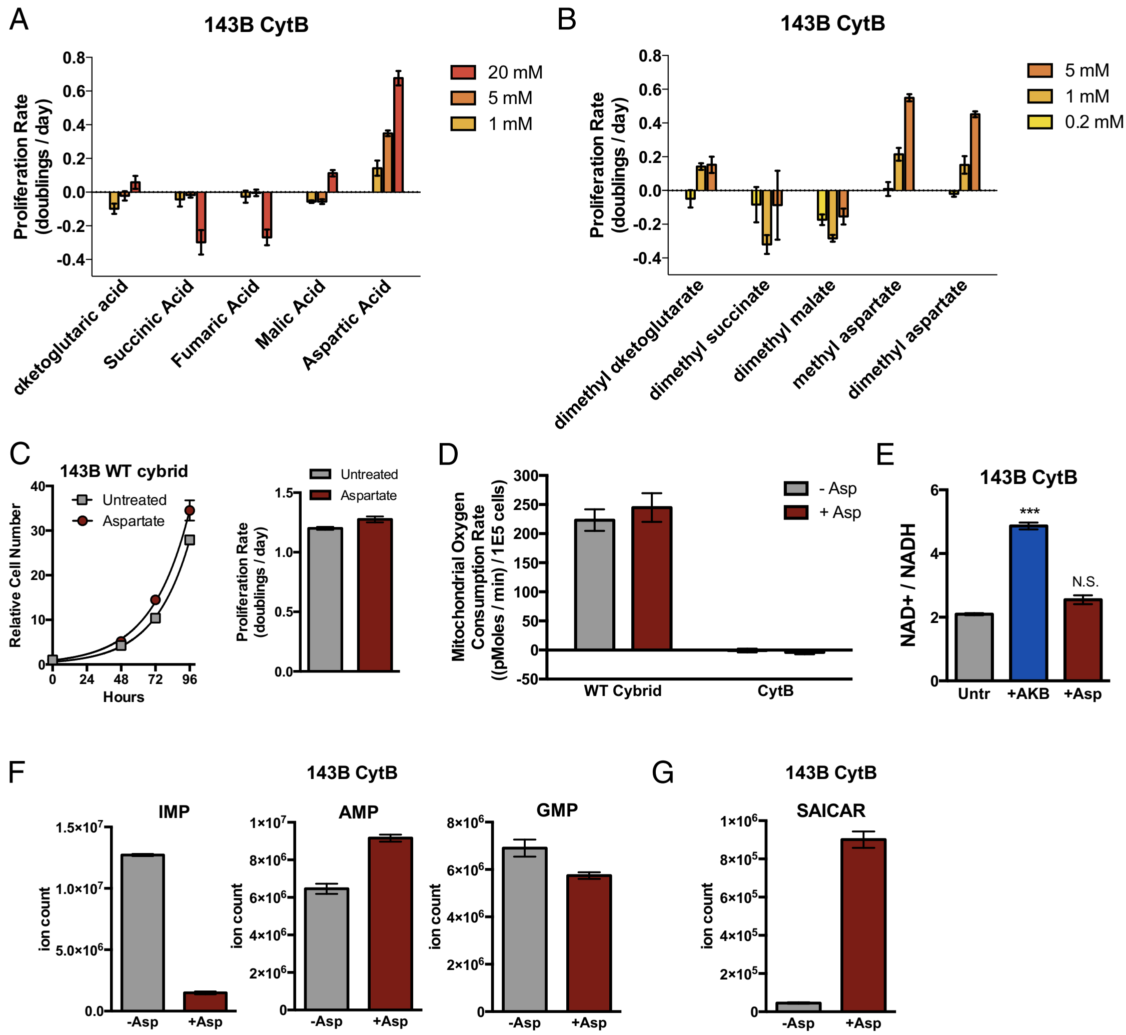

Figure S5. Aspartate Supplementation Restores Adenine Nucleotide Levels and Supports Proliferation Without Affecting NAD+/NADH or Oxygen Consumption, Related to Figure 6

(A) Proliferation of 143B CytB cells determined after supplementation with the indicated concentrations of TCA-cycle intermediates or aspartic acid. (B) Proliferation of 143B CytB cells was determined after supplementing with the indicted concentrations of methyl ester derivatives of TCA-cycle intermediates or aspartate. (C) Proliferation of 143B WT cybrid cells was determined in the presence or absence of aspartate. (D) Mitochondrial oxygen consumption rate was determined in 143B WT Cybrid and 143B CytB cells in the presence or absence of aspartate. (E) Intracellular ratio of NAD+/NADH measured in 143B CytB cells cultured in standard media (Untr) or in media supplemented with AKB or aspartate (Asp). (F) LCMS quantification of purine nucleotide levels in 143B CytB cells without or with aspartate supplementation. (G) LCMS quantification of SAICAR levels in 143B CytB cells cultured without or with aspartate supplementation. Values in all figures denote mean ± SEM, n = 3 (A-C, E-G), n = 5 (D). *** represents $p \leq 0.001$, N.S. indicates the measured values were not statistically different ($p > 0.05$).

Cell

Supplemental Information

Supporting Aspartate Biosynthesis Is an Essential Function of Respiration in Proliferating Cells

Lucas B. Sullivan, Dan Y. Gui, Aaron M. Hosios, Lauren N. Bush, Elizaveta Freinkman, Matthew G. Vander Heiden

Supplemental Experimental Procedures

Proliferation Rates

Adherent cell lines growing in log phase were trypsinized, counted, and plated onto 6 well dishes (Corning) in 2 mL complete DMEM and incubated overnight. Initial seeding density was 20,000 cells per well for 143B, A172, H1299, HeLa, 143B WT Cybrid, and MEFs and 30,000 cells for 143B CytB and U87 cells. The following day, one plate of cells was counted to determine starting cell number at the time of treatment. Cells were washed 2 times with 2 mL phosphate buffered saline (PBS) and 4 mL media premixed with the indicated metabolites or compounds was added. FL5.12 cells, a suspension cell line, were washed 2 times in PBS and added directly to IL-3-containing media with the indicated metabolites or compounds. Proliferation rates were measured in DMEM without pyruvate containing 10% dialyzed fetal bovine serum, penicillin-streptomycin, and 0.1 mg/mL uridine, unless otherwise noted. For all conditions the seeding densities used allowed exponential proliferation for 4 days and final cell counts were measured 4 days after treatment. Cells were counted using Cellometer Auto T4 Plus Cell Counter (Nexcelom Bioscience). Proliferation rate was determined using the following formula:

$$\text{Proliferation Rate (Doublings per day)} = \log_2 \text{(Final cell count (day 5)/Initial cell count (day 1))/4 (days)}$$

Concentrations of all metabolites and compounds added to culture media for each cell line are included as a table in supplemental methods (Table S1).

Mitochondrial Oxygen Consumption

Oxygen consumption rates were determined using a Seahorse Bioscience Extracellular Flux Analyzer (XF24). Cells were plated in Seahorse Bioscience 24 well plates at 60,000 cells per well in 100 µl complete DMEM, allowed to attach for 1 hour, and 500 µl complete DMEM was added before overnight incubation.

The following day cells were washed 2 times in assay media: DMEM without phenol red or pyruvate containing 0.5% dialyzed FBS and 0.1 mg/mL uridine at pH 7.4 and incubated in 500 µL of the same media. Oxygen consumption measurements were compared between basal measurements and following injection of the compound (AKB, rotenone, antimycin), or between wells cultured overnight in their treatment conditions (aspartate, oligomycin, FCCP). These measurements were then subtracted from oxygen consumption measurements following addition of high dose rotenone and antimycin treatment (2 µM each) to determine the mitochondria specific oxygen consumption rate. Following measurements, cell number was determined, averaged per condition, and the mitochondrial oxygen consumption rates were normalized to 100,000 cells.

Lactate Dehydrogenase Assay

Immediately prior to the start of the assay 100 *µ*l of a reaction buffer containing 50 mM HEPES-KOH pH 7.5, 20 mM KCl, 2 mM $MgCl_2$, 1 mM DTT, 180 *µ*M NADH, 1 mM alpha-ketobutyrate (when used) was combined with LDH (Sigma) (when added) in 96-well plates. Lactate dehydrogenase activity was assayed by monitoring disappearance of NADH absorbance at 340 nm over time.

Viability

Cell viability was determined by propidium iodide (PI) exclusion by standard protocols. 143B WT cybrid and HeLa cells were seeded overnight at 50,000 cells per well on 6 well plates. The following day, cells were washed 2 times with PBS and complete DMEM or DMEM without glucose, glutamine, or pyruvate was added with the indicated supplements. After 48 hours (HeLa) or 72 hours (143B WT Cybrid) both attached and suspension cells were collected and resuspended in 1 *µ*g/ml PI. PI incorporation was measured by flow cytometry (BD FACS Canto II) and quantified (FACS Diva Software).

Purine Nucleotide Metabolite Extraction and LCMS Analysis

143B CytB cells were seeded at 400,000 cells/well in 6 well dishes overnight. The following day, cells were washed 2 times in PBS and media was changed to proliferation assay media with or without the indicated treatments. After 15 hours, polar metabolites were extracted from cells using 250 μl of ice cold 80% methanol. After scraping the cells, 250 μl of chloroform was added before vortexing for 10 min at 4 °C and centrifugation for 10 min at 4 °C at 16,000g. 40 μl of the top, water-methanol layer was transferred into a LCMS tube prior to sample analysis. A Dionex UltiMate 3000 ultra-high performance liquid chromatography system connected to a Q Exactive benchtop Orbitrap mass spectrometer, equipped with an Ion Max source and a HESI II probe (Thermo Fisher Scientific) was used to quantify metabolites. Samples were separated by chromatography by injecting 10 μl of sample on a SeQuant ZIC-pHILIC Polymeric column (2.1 × 150 mm 5 µM, EMD Millipore). Flow rate was set to 150 μl/min, temperatures were set to 25 °C for column compartment and 4 °C for autosampler sample tray. Mobile Phase A consisted of 20 mM ammonium carbonate, 0.1% ammonium hydroxide. Mobile Phase B was 100% acetonitrile. The mobile phase gradient (%B) was set in the following protocol: 0-20 min.: linear gradient from 80% to 20% B; 20-20.5 min.: linear gradient from 20% to 80% B; 20.5-28 min.: hold at 80% B. Mobile phase was introduced into the ionization source set to the following parameters: sheath gas = 40, auxiliary gas = 15, sweep gas = 1, spray voltage = –3.1kV, capillary temperature = 275 °C, S-lens RF level = 40, probe temperature = 350 °C. Metabolites were monitored using full scan in negative mode in the range of 285-700 m/z, with the resolution set at 140,000, the AGC target at 1,000,000, and the maximum injection time at 250 msec. Relative quantitation of metabolites was performed with XCalibur QuanBrowser 2.2 (Thermo Fisher Scientific) using a 5 ppm mass tolerance and referencing an in-house retention time library of chemical standards.

Measurement of NAD+/NADH

NAD+/NADH measurements were done using a modified version of manufacturer instructions supplied with the NAD/NADH Glo Assay (Promega). Cells were plated as done for proliferation assays and treated as indicated prior to preparation of cell extracts 6 hours after treatment. For extraction, cells were washed 3 times in ice cold PBS, extracted in 100 µL ice cold lysis buffer (1% Dodecyltrimethylammonium bromide (DTAB) in 0.2 N NaOH diluted 1:1 with PBS), and immediately frozen at -80°C. To measure NADH, 20 µL of sample was moved to PCR tubes and incubated at 75°C for 30 min where basic conditions selectively degrade NAD+. To measure NAD+, 20 µL of the samples was moved to PCR tubes containing 20 µL lysis buffer and 20 µL 0.4 N HCl and incubated at 60°C for 15 min, where acidic conditions selectively degrade NADH. Following incubations, samples were allowed to equilibrate to room temperature and then quenched by neutralizing with 20 µL 0.25 M Tris in 0.2 N HCl (NADH) or 20 µL 0.5 M Tris base (NAD+). Manufacturer instructions were followed thereafter to measure NAD+/NADH.

Statistical Analysis

Data are presented as the mean ± standard error of the mean (SEM). Sample size (n) indicates experimental replicates from a single representative experiment, the results of all experiments were validated by independent repetitions. Statistical significance was determined using a two-tailed Welch's t test where significance is $p \leq 0.05$.

Table S1. Concentrations of Media Supplements and Inhibitors Used, Related to Experimental Procedures.

Unless otherwise noted, the concentrations of all compounds were as follows:

Cell Line	AKB (mM)	Asp (mM)	Rot (nM)	Ant (nM)	Oligo (nM)	Phen (μM)	Myxo (μM)	N_3 (μM)	FCCP (nM)
143B	1	20	30	100	5	20	5	600	250
A172	1	10	75	2000	1				
H1299	1	10	50	5000	1				
HeLa	1	20	30	800	1				
MEF	1	20	200	10000	3				
FL5	1	20	30	500	0.5				
U87	1	20	40	250	5				
143B CytB	1	20							
143B WT cybrid	1	20							

Abbreviations: AKB, alpha-ketobutryate; Asp, aspartate; Rot, rotenone; Ant, Antimycin; Oligo, Oligomycin; Phen, phenformin; Myxo, Myxothiazol; N_3, Sodium Azide; FCCP, Carbonyl Cyanide-4-(Trifluoromethoxy) Phenylhydrazone.